Research Article **Open Access**

Marcia Ernesto*, Piero Comin-Chiaramonti, and Celso de Barros Gomes

The Early Triassic magmatism of the Alto Paraguay Province, Central South America: Paleomagnetic and ASM data

DOI 10.1515/geo-2015-0022
Received Mar 24, 2014; accepted Feb 23, 2015

Abstract: A paleomagnetic studystudywork was carried out on the Alto Paraguay Province (APP), a belt of alkaline complexes that parallel the Paraguay river for more than 40 km at the border of Brazil and Paraguay. The province is well dated by ^{40}Ar/^{39}Ar method giving ages in the range 240–250 Ma with a preferred age of 241 Ma. Intrusive rocks are predominant but the stocks may be topped by lava flows and ignimbrites. Paleomagnetic work on stocks, dikes and flows of the APP identified normal and reversed magnetic components which are carried mainly by titanomagnetites. The calculated paleomagnetic pole located at 319°E 78°S (α_{95} = 6°; k = 23) is in agreement with other South American poles of Permo-Triassic age. Most of the sampling sites showed large variations in rock magnetization, but similar patterns in the variation of the within-site magnetizations, mainly in dikes, suggest geomagnetic polarity transition records. The magnetization data along with the anisotropy of magnetic susceptibility determinations suggested that the South and North areas of the province have different evolution characteristics.

Keywords: alkaline magmatism; paleomagnetism; magnetic anisotropy; Alto Paraguay Province

1 Introduction

The cratonic area of South America experienced an epoch of quiescence since Cambrian times favoring the onset of large intracratonic sedimentary basins as was the case of the Paraná Basin [1, 2]. In this basin there is no record of magmatic activity up to Early Cretaceous when an huge flood basalt volcanism [3] covered the entire area. A subsequent intrusive magmatism of alkaline nature is recognized all around the present limits of the basin [4]. However, on the western border of the basin, alkaline complexes belonging to the Alto Paraguay Province (APP) [5] are as old as Early Triassic.

The geodynamic context of the APP magmatism has been related either to the Rio Apa Arch [6] occurring westwards of the province or to the activation of the Alto Paraguay N-S structures. A genetic relationship between the APP rocks and the Cabo-La Ventana (Pampean) orogeny was proposed [7] following other analogous suggestions [8–11]. On the basis of magnetotelluric soundings and gravimetric data, [12] also proposed the continuation of the Pampean belt under the Pantanal sedimentary cover as the Paraguay belt. According to [13, 14], small ancient crustal blocks at the present-day Paraguay boundaries were continuously reworked. In this context, [15] suggested that the APP Na-alkaline magmatism occurred at the boundaries between the Rio Apa and Arequipa-Antofalla blocks as a result of the extensional regimes derived from the relative movements of the ancient blocks.

The dynamics of magma pulses and growth of magma bodies has been the focus of an increasing number of studies (recent overviews in Tectonophysics 500, 2011), and new geological, geophysical and geochronological informations may bring new insights for the pluton build up models. In this paper we present paleomagnetic and anisotropy of magnetic susceptibility investigations aiming to contribute to better understanding the emplacement context of the APP rocks.

2 Geological background

The Paraná Basin is a large cratonic basin occupying southern Brazil and adjacent areas in Argentina,

***Corresponding Author: Marcia Ernesto:** Department of Geophysics, University of São Paulo, Rua do Matão 1226, 05508-090 São Paulo, SP, Brazil; Email: mernesto@usp.br
Piero Comin-Chiaramonti: Department of Mathematics and Geosciences, University of Trieste, Via Weiss 2, 34127 Trieste, Italy; Email: comin@units.it
Celso de Barros Gomes: Institute of Geosciences, University of São Paulo, Rua do Lago, 05508-080 São Paulo, SP, Brazil; Email: cgomes@usp.br

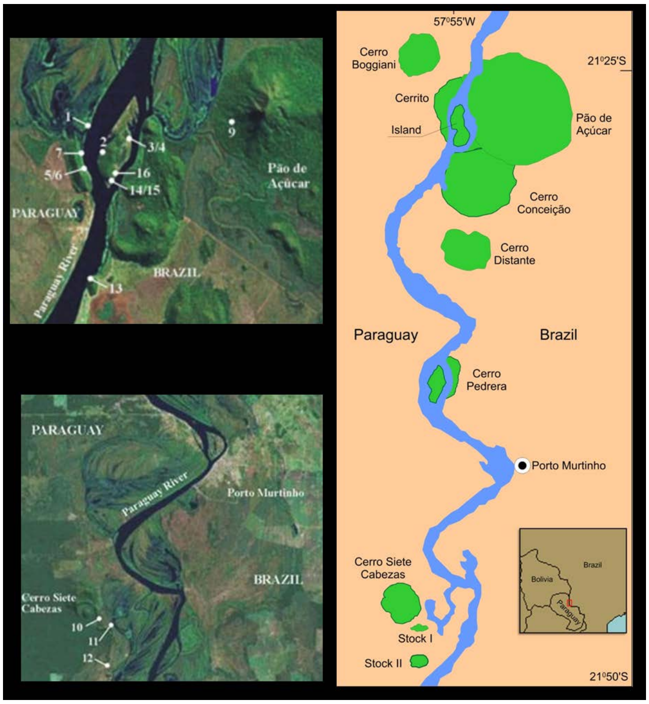

Figure 1: Location maps of the sampling sites. The sketch map [7] displays the location of the complexes; sampling sites are indicated on the left (South area) and right (North area) images.

Paraguay, and Uruguay. The sedimentary filling of the basin started in the Ordovician and extended until the Early Cretaceous when extensive extrusivea huge flood? magmatic activity covered the entire basin [1, 3]. Sills and dikes also of Early Cretaceous age are widespread all over the basin, and cut mainly the upper Paleozoic to Cretaceous sedimentary rocks ([e.g. 2]). Dike swarms surround the basin, and younger ages tend to concetrate to the north where Late Cretaceous intrusive alkaline magmatism also becomes more abundant.

However, in the Brazil-Paraguay border an older alkaline magmatism of Triassic age dominates landscape for nearly 40 km along the Paraguay River (Fig. 1). This area, located at 21°00'–23°35'S and 57°10'–58°00'W, is referred to as Alto Paraguay Province (APP) and comprises a series of stocks and ring complexes cropping out to the north and south of Porto Murtinho, the most important city in the region. Alkaline rocks occur associated with sediments of the Pleistocenic Pantanal Formation which covers the Chaco-Pantanal system [1]. The Pantanal Basin is an elongated N–S feature in central-west Brazil and has been formed as a consequence of the Andean orogeny [16, 17]. The plain developed over metamorphic rocks of the Alto Paraguay folded belt; its structural features have been reactivated since the late Pleistocene imprinting NE and NS structural directions in the plain [18].

Seven major circular complexes are described in the APP [7, 19]: Cerro Siete Cabezas, Cerro Pedreira, Morro Distante, Morro Conceição, Fecho dos Morros, Pão de Açúcar and Cerro Boggiani; the stocks are cut by dikes, and may be topped by lava flows. The complexes are mostly sodic in composition and mainly represented by nepheline syenites and syenites, and quartz-bearing syenitic rocks subordinately; phonolites, trachyphonolites, trachytes, rhyolites and ignimbrites are the principal fine-grained rocks. Phonolitic lava flows are occasionally found on the top of hills as noted in the Pão de Açúcar complex. From a petrochemical point of view, two main suites are apparent for the APP alkaline rock-types [7]: an agpaitic, strongly undersaturated in silica and peralkaline suite is dominant in the Cerro Boggiani, Pão de Açúcar and Cerrito complexes, whereas a suite tending to miaskitic and oversaturated prevails in the Cerro Siete Cabezas complex.

From a petrochemical point of view, two main suites can be defined within the group of the alkaline rock-types (Fig. 3). An agpaitic, strongly undersaturated suite is dominant in the north (Cerro Boggiani, Pão de Açúcar and Cerrito complexes), while a predominantly miaskitic and oversaturated suite is found in the Cerro Siete Cabezas complex.

The APP is well dated by different radiometric methods. K-Ar ages are in the range ~228–255 Ma [20–22]; in the northern APP two Rb-Sr isochron gave ages of 255±11 Ma [22], and Ar^{39}/Ar^{40} determinations done on different minerals and whole rock presented values varying from 236 to 250 Ma [22]. However, on the basis of plateau ages for biotite separates from samples of different complexes, a significant less broad interval of ages (240.6±0.4 to 241.9±0.4 Ma) was provided [15]; a mean age of 241.5±1.3 Ma was suggested to characterize the whole province. Particularly, an integrated age of 242.0±1.6 Ma was obtained for the Pão de Açúcar rocks [5, 7], which is well in accordance with the age interval for the entire APP.

3 Paleomagnetic data

Samples from 22 independent paleomagnetic sites (15 localities, cf. Fig. 1) were collected from the river banks where fresh *in situ* rocks are exposed. The sampling sites (Table 1) include stocks (13 sampling sites), seven dikes which were seen mainly in the North area, and two lava flows (sampling point 9) from the Pão de Açúcar hill.

Samples were taken with the aid of a portable gasoline powered drill; normally four to five cylinders were cut and oriented by both magnetic and sun compasses. Specimens

Table 1: Location and description of the sampling sites.

Locality	Complex[1]	Latitude (°S)	Longitude (°W)	Sampling point	Observations
North area					
1	Cerrito	21°27'06"	57°55'41"	505	Stock
1	Cerrito	21°27'06"	57°55'41"	506	Dike N276/85; width=10 cm
2	Island	21°27'06"	57°55'33"	507	Stock
3	Island	21°26'55"	57°55'05"	508	Stock
4	Island	21°27'17"	57°55'39"	509	Stock
4	Island			510	Dike; width=30cm
5	Fecho dos Morros	21[]°27'20"	57[]°55'39"	511	Stock and fine grain band with phenocrystals
6	Fecho dos Morros	21°27'18"	57°55'43"	512	Dike N98/vertical;
7	Fecho dos Morros	21°27'08"	57°55'53"	513	Stock
8	Cerro Pedreira	21°36'03"	57°55'04"	514	Stock
9	Pão de Açúcar	21°26'33"	57°55'30"	516	Flow; height=240 m
9	Pão de Açúcar	21°26'33"	57°55'30"	517	Flow; height=250 m
13	Fazenda Cerrito	21°28'29"	57°55'41"	522	Stock
14	Island	21°27'23"	57°55'26"	523	Stock
14	Island	21°27'23"	57°55'26"	524	Dike N280/vertical; width=30cm
15	Island	21°27'23"	57°55'21"	525	Dike N280/vertical; width=4m
15	Island	21°27'25"	57°55'26"	526	Dike N310/45NE; width=1m
15	Island	21°27'25"	57°55'26"	527	Dike
15	Island	21°27'25"	57°55'26"	528	Stock
South area					
8	Cerro Pedrera	21°36'03"	57°55'11"	515	Dike, N303/vertical; width=25–40cm
10	Stock I	21°47'23"	57°57'09"	518	Stock
11	Cerro Siete Cabezas	21°47'20"	57°57'13"	519	Stock
12	Stock II	21°48'54"	57°57'04"	520/521	Stock

[1] As named in [7].

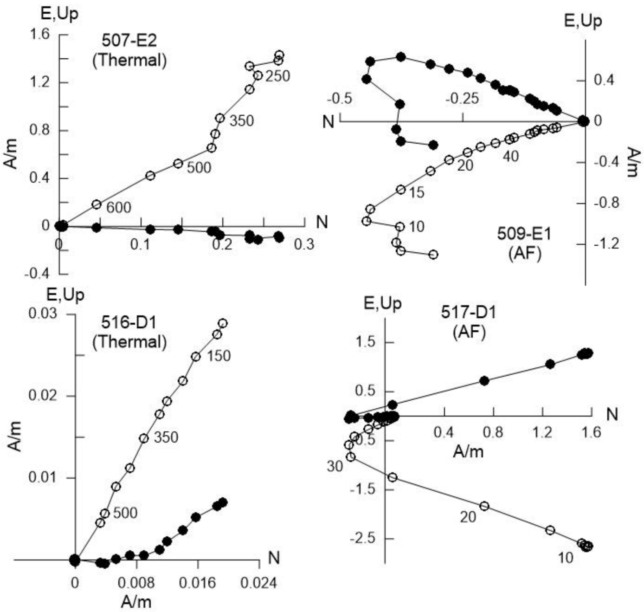

Figure 2: Orthogonal plots for some samples during thermal and AF demagnetization. Open (full) symbols are vertical (horizontal) projections.

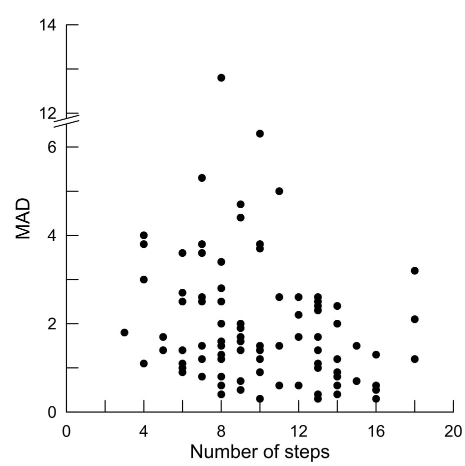

Figure 3: The MAD parameter for the high coercivity components of magnetization as a function of the number of AF demagnetization steps.

of one inch in diameter and 2.2 in height were prepared, and submitted to both alternating field and thermal demagnetizations generally up to 120 mT or 600°C (few samples up to 680°C). During thermal demagnetization the most stable (higher unblocking temperatures – T_{ub}) components were revealed mainly in the range 250–600°C.

In general samples showed high coercivity (Hc) components which were erased above 80 mT (Fig. 2); low coercivity components were isolated at fields lower than 15mT medium; a third component of medium coercivity in the range ~15–30 mT was detected in some samples. The Hc

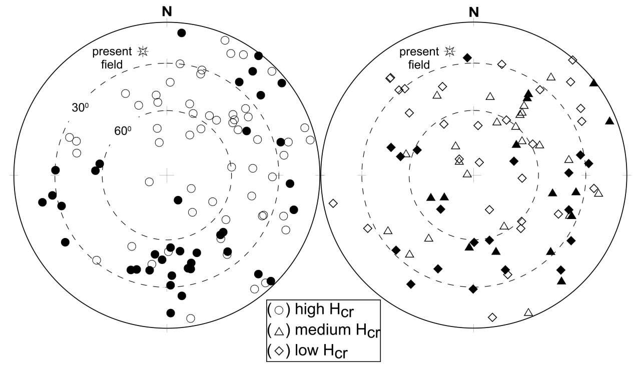

Figure 4: Stereograms displaying all the identified high (left) and medium to low (right) coercivity/unblocking temperature magnetization components. Open (full) symbols represent negative (positive) inclinations.

magnetization components were very well defined, and the maximum angular deviation (MAD) was normally less than 4 for 7 to 11 consecutive steps in most cases (Fig. 3). However, the within-site dispersion of the most stable components was too large, and not all sites gave reliable (statistical parameter α_{95} [24] < 30°) mean magnetization directions. Table 2 displays site-mean directions for sites with at least three congruent results.

The same dispersion observed for the Hc components (Fig. 4) is observed for the low and medium Hc components (Fig. 4). in Fig. 4 all the identified components for individual specimens are represented and very few data plot close to the present field direction, indicating that the magnetization was hard enough to prevent alterations by the present field induction effect. A closer look to the magnetization dispersion for various sites (Fig. 5) suggests that the dispersion is not random but follow a pattern that may be related to changes of the magnetizing field. In the dike 526 (Fig. 5a) the magnetization varies from the border to the center (faster to slower cooling) tending to a shallower positive inclination. Same behavior is seen in sites 505 and 511; in the latter, most of the samples have positive inclinations and the more mafic band (specimen 511C in Fig. 5), which corresponds to a younger record, has negative inclination. This behavior may represent the records of a transitional geomagnetic field. Various other sites apparently display the same pattern (Fig. 5c), but unfortunately the data cannot be organized in chronologic order.

The two investigated flows also indicate a transition from normal (lower flow) to reversed (upper flow) polarity (Fig. 5b). Furthermore, the magnetization of the reversed flow shows a variation from bottom to top suggesting the record of the final stages of a polarity transition. The virtual geomagnetic poles (VGP) calculated for each specimen are distributed from south to north, and mainly con-

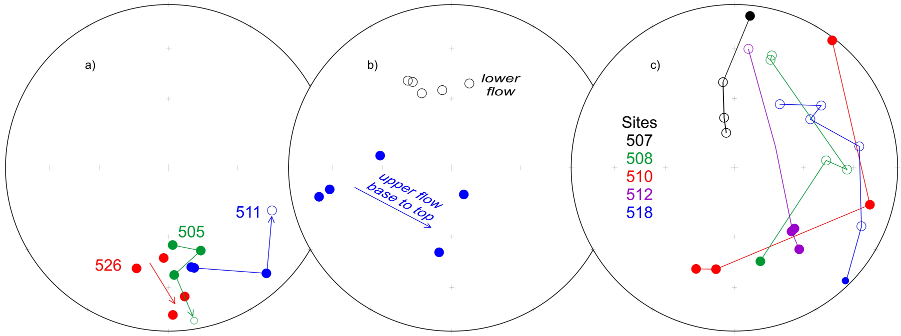

Figure 5: Within-site dispersion of the Hcr remanaent magnetization of some sampling sites; symbols indicate positive (full symbols) and negative (opens symbols) inclinations; a) sites with chronological control; the arrows point to the youngest magnetizations; b) variation of the magnetization within the two flows; c) results of some sampling sites showing large dispersion but with no chronological control.

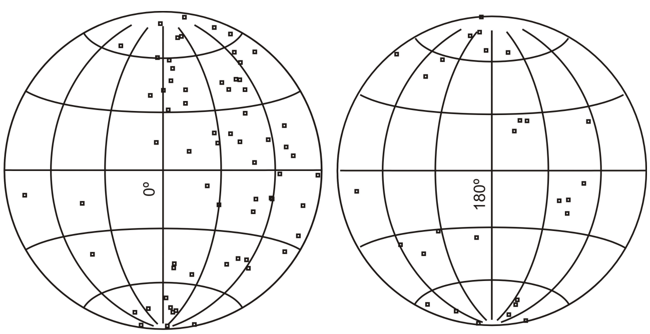

Figure 6: Virtual geomagnetic poles corresponding to the Hcr component of all specimens.

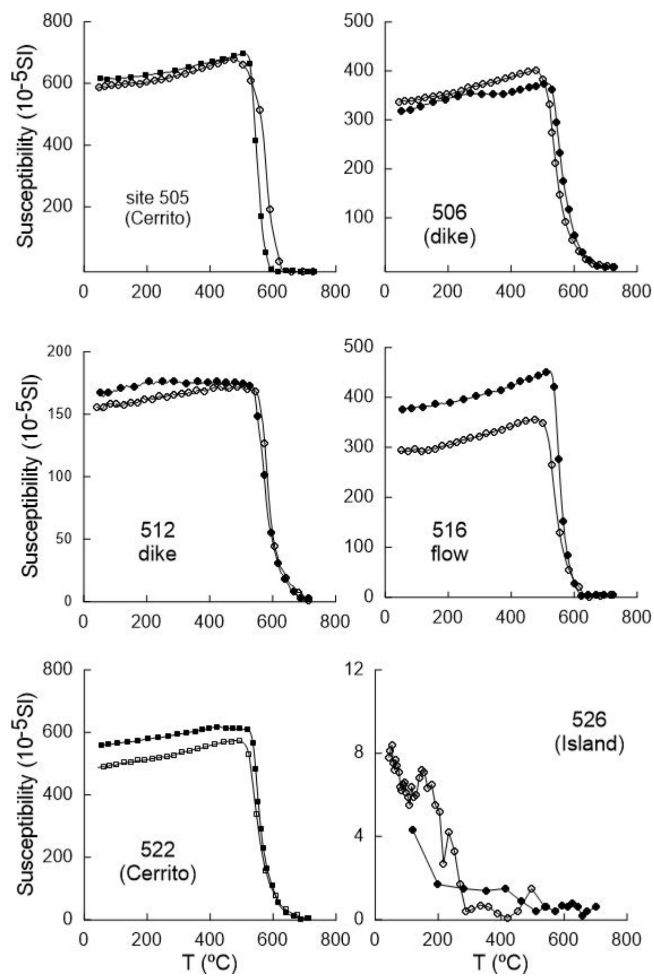

Figure 7: Thermomagnetic curves (k versus T) for samples from different sampling sites during heating (full symbols) and cooling (open symbols). The curves indicate titanomagnetite as the main magnetic carrier.

centrated within the 30–90° longitude band (Fig. 6). This distribution may represent the path of the geomagnetic field during polarity changes, as indicated by the analysis of the remanent magnetizations.

4 Rock magnetism and AMS

Reversible thermomagnetic curves (Fig. 7) are typical for almost all sampling sites, and suggest titanomagnetite with low Ti-content as the main magnetic carrier. Under reflected light microscopy titanomagnetites in the flow samples exhibited structures related to high temperature oxidation and ilmenite exsolution. In most of the sampling sites fine grains of titanomagnetite are spread over the matrix. Eventually some hematite is present, as well as small quantities of maghemite, as seen in the curve of site 506. The isothermal remanent magnetization (IRM) acquisition curves (Fig. 8) indicate high coercivity minerals normally saturating at fields of at least 100 mT. This behavior is indicative of fine magnetite grains of high coercivities.

In general the APP rocks have a low degree of anisotropy of magnetic susceptibility (AMS) with values concentrated in the range 1.02–1.06 (Fig. 9). Bulk suscepti-

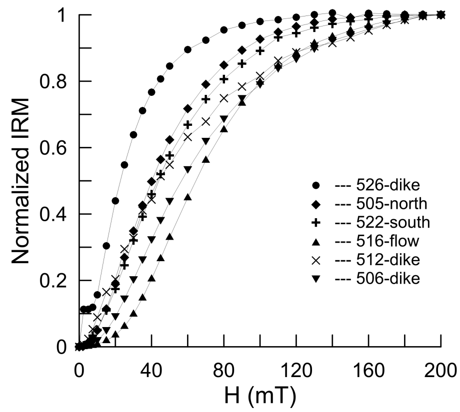

Figure 8: Isothermal remanent magnetization curves for samples of different sites.

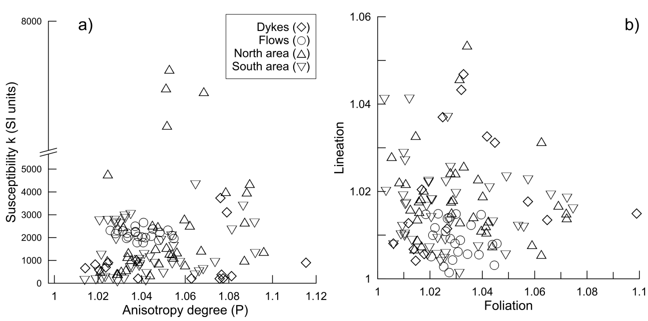

Figure 9: a) Variation of magnetic susceptibility as a function of the anisotropy degree (k1/k3), and b) the magnetic lineation (k_1/k_2) versus the magnetic foliation (k_2/k_3). Data refers to individual specimens.

bilities concentrate over a narrow range, but some higher values are noticed in the North area. The magnetic fabric is either of lineated and foliated character however, foliation prevails in the flows; in general, foliated fabric mimics the magma flow.

AMS determinations were performed before submitting the specimens to magnetic cleaning. The three main anisotropy axes (k_1, k_2 and k_3) determined for flows, dikes and stocks are displayed in the stereograms of Fig. 10. The two flows show the major axes k_1 and k_2 distributed on a subhorizontal plane (k_1 inclinations ≤ 30°). The mean $k_3$direction corresponds to the pole to the foliation plane defined by the major axes. It is currently admitted that the $k_1$directions mark the magma flux ([e.g. 27, 28]) in lava flows. The dikes show mainly subvertical k_1 axes, but also subhorizontal k_1 axes are present as seen on the examples of Fig. 10. The stocks tend to give steep k_1 axes mainly in the outcrops of the North area. In the South area k_1 inclinations are more variable and describes a N-S trend; however, most of the k_1 axes still have inclinations ≥ 60°, indicating proximity of the magma sources.

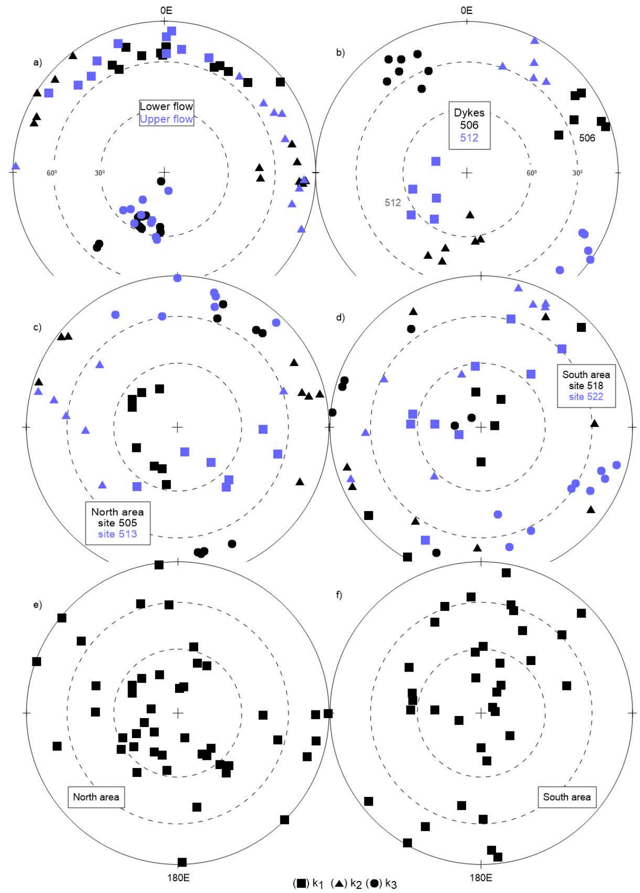

Figure 10: a) Distribution of the AMS main axes (k_1, k_2 and k_3) for the two flows; b) examples of the AMS axes in dikes; c) and d) k_1 and k_2 axes in the stocks of the North and South areas, respectively.

The above characteristics and the low degree of anisotropy observed for the majority of the APP rocks, suggest that the area were not affected by intense stresses after the emplacement of the magmatic province.

5 Discussion

The paleomagnetic pole based on the site mean magnetizations of the more stable sites (Table 2) is located at 318°E 79°S (N=7; α_{95} = 14.5°; k = 18) and is in agreement with other Late-Permian to Triassic poles for South America. However, this pole is mainly based on the results of flows and dikes; if we give unit weight to specimens it is possible to calculate a paleomagnetic pole which includes information from the other sites that gave no reliable means. This procedure, however, does not change significantly the paleomagnetic pole (Table 2) but gives better statistical parameters as it enlarges the dataset. Two different cut offs

Table 2: Paleomagnetic results for the APP rocks.

	Mean Magnetization Direction					VGPs	
Sampling sites	Dec. (°)	Inc. (°)	N	α_{95} (°)	k	PLong. (°E)	PLat. (°S)
505	171.2	47.8	3	17.4	51	347.3	−79.1
506	29.3	−64.2	3	9.6	17	264.8	−55.8
507	350.2	−65.2	3	20.3	38	316.8	−63.0
508	8.5	−37.2	3	26.0	24	208.8	−82.0
512	152.5	45.1	4	24.5	15	14.9	−64.4
513*	58.2	−51.9	3	21.2	35	237.3	−37.6
516	345.5	−50.6	5	11.0	49	351.7	−73.7
518	50.1	−47.5	3	17.6	50	231.4	−44.5
526	182.3	30.8	4	21.7	19	146.6	−84.7
527*	109.3	−45.4	4	28.7	11	64.2	−6.3
Mean (unit weight per site)	183.3	48.9	7	15.8	15	318	−79
					(N = 7; α_{95} = 14.5; k = 18)		
Mean (cut off=30°; unit weight per specimen)						319	−78
					(N = 26; α_{95} = 6.0; k = 23)		
Mean (cut off=45°; unit weight per specimen)						292	−83
					(N = 41; α_{95} = 6.8; k = 12)		

Dec. and Inc., Declination and Inclination;
N, number of site/specimens for mean calculations;
α_{95} and k, Fisher's [24] statistical parameters

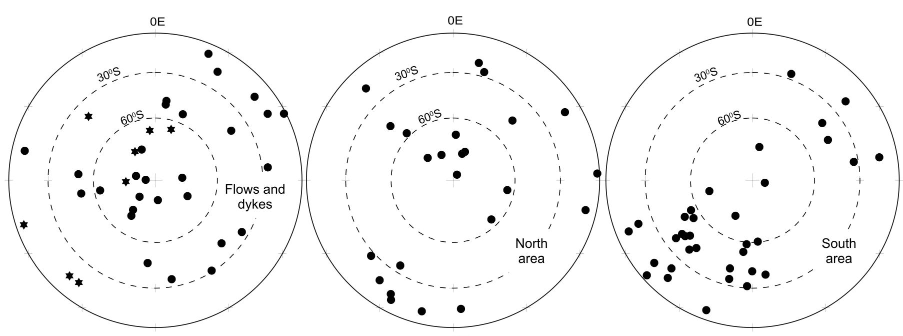

Figure 11: VGP distributions for dikes (circles) and flows (stars), and for the North and South areas. VGPs refer to individual specimens based onand their most stable components (high coercivities or high unblocking temperatures), and are seen from the South geographic pole.

were used (30° and 45°) to calculate the mean of PGVs, which resulted in similar results considering the statistical uncertainties. The preferred pole is at 319°E 78°S (N = 26; α_{95} = 6.0°; k = 23) which is closer to the mean of the most reliable sites. The mean pole for South America for the interval 200-250 Ma compiled by [25] is at 295°E 79°S (N = 3; α_{95} = 9.5°) and matches well the APP pole.

One problem in calculating a paleomagnetic pole from the APP rocks is the lack of reference planes to estimate possible tilting. The subhorizontal foliation planes given by the AMS measurements of the flows may give an indication of the paleohorizontal. The mean of the minimum axes k_3 (the pole to the foliation plane) directions suggest a dip of 24° to N205°, and such a bedding correction would displace the APP paleomagnetic pole to a position (157°E 80°S), if taken as representative of the entire igneous province. This pole position is close to the Late Jurassic segment of the apparent polar wander path for South America [29], and would imply in a remagnetization of the entire province, for which there isare no evidences from the paleomagnetic and the rockmagnetic data described above. Therefore, if the maximum axes k_1 are really parallel to the flow direction it is possible that the foliation plane refers only to the Pão de Açúcar complex or it means that the emplacement surface was not horizontal. Strong evidence against the hypothesis of remagnetization is given by sampling point 1 where the host-rock (sample 505) has a reversed magnetization as shown in Fig. 5, whereas the cutting dike (sample 506) is of normal polarity (Table 2). The dike is only 10 cm thick, and therefore, an influence of the intrusion to the magnetization of the host-rock must be discarded.

The remaneant magnetizations suggest that at least three polarity intervals were recorded by the complexes. A mean duration of 0.53 m.y. and a corresponding reversal rate of 1.88/m.y. was estimated for the Late Triassic [30]. Therefore, a few million years may be assumed to accomplish for the magnetic records of the investigated rocks if that estimate is also valid for the Early Triassic.

The distributions of the VGPs for the North and South areas (Fig. 10) have the same NE-SW tendency but for the South area they are concentrated in the 180-270° quadrant and at latitudes lower than 60°S. This distribution contrasts to the one for the North area which includes the flows and the dikes, except one. The AMS also shows different patterns in the two areas (Fig. 11): k_1 axes are steeper and trend NW-SE in the North area, whereas in the South area they trend N-S. These differences are related to distinct modes of construction of the plugs, and/or indicate that the two areas have been submitted to different stress fields. This is in accordance with previous observations based on the AMS data.

6 Concluding remarks

The Alto Paraguay Province consists of a series of ring complexes forming a narrow N-S band that parallel the Paraguay River for more than 40 km at the border of Brazil and Paraguay. Intrusive rocks are predominant, except for the Pão de Açúcar complex which corresponds to a volcanic field. The province is well dated by Ar/Ar method with a preferred age of 241 Ma [15, 31].

The remaneant magnetization of the APP rocks is mainly carried by high coercive magnetite. Characteristic components of magnetization include both normal and reversed polarities, but also an abnormally large number of anomalous directions which can be related to polarity transitions. The calculated paleomagnetic pole along other Late-Permian to Early Triassic poles places South America in a position that favors the A-type reconstruction of Pangea [cf. 32, 33]. Magnetic anisotropy indicates subhorizontal foliated fabric for lava flows which may be related to original magma fluxes. For the stocks the main susceptibility k_1 axes delineate planes in approximately N-S (South area) and NW (North area) directions; however, steep inclinations are predominant indicating proximity to the magma sources.

Acknowledgement: Thanks are due to Daniele Brandt for her help in various laboratory routines. This work was funded by the Brazilian agencies FAPESP and CNPq.

References

[1] Fúlfaro V.J., Geology of Eastern Paraguay. In: Comin-Chiaramonti, P., Gomes, C.B. (Eds.), Alkaline magmatism in central-eastern Paraguay. Relationships with coeval magmatism in Brazil, Edusp/Fapesp, São Paulo, 1996, pp. 17-30.

[2] Zalán P.V., Wolff S., Astolfi M.A., Santos V.I., Conceição J.C., Appi V., Neto E.V.S., Cerqueira J.R., Marques A., The Paraná basin, Brazil. In: Leighton, M.W., Kolata, D.R., Olttz, D.F., Eidel, J.J. (Eds.), Am. Assoc. Petroleum Geol., Memoir, 51:681–703, 1990.

[3] Piccirillo E.M., Melfi A.J. (Eds.), The Mesozoic flood volcanism from the Paraná basin (Brazil), Petrogenetic and geophysical aspects, IAG-USP, 1988, 600p.

[4] Comin-Chiaramonti P., Gomes C.B. (Eds.), Mesozoic to Cenozoic alkaline magmatism in the Brazilian Platform, Edusp/Fapesp, São Paulo, 2005, 752p.

[5] Velázquez V.F., Gomes C.B., Orué D., Comin-Chiaramonti P., Magamatismo alcalino do Paraguai: uma revisão e atualização das províncias, Bol. IG-USP, Sér. Cient., 26:61–79, 1996.

[6] Livieres R.A., Quade H., Distribución regional y asentamiento tectónico de los complejos alcalinos del Paraguay, Zentr. Geol. Paläontol., 7/8:791–805, 1987.

[7] Comin-Chiaramonti P., Gomes C.B., Censi P., Gasparon M., Velázquez V.F., Alkaline complexes from the Alto Paraguay Province at the border of Brazil, Mato Grosso do Sul State) and Paraguay. In: Comin-Chiaramonti P., Gomes, C.B. (Eds.), Mesozoic to Cenozoic alkaline magmatism in the Brazilian Platform., Edusp/Fapesp, São Paulo, 2005, pp. 71–148.

[8] Tankard A.J., Uliana M.A., Welsink H.J., Ramos V.A., Turic M., França A.B., Milani E.J., Brito Neves B.B., Eyles N., Skarmeta J., Santa Ana H., Wiens F., Cirbián M., Paulsen O.L., Germs G.J.B., De Wit M.J., Machacha T., Miller R., Structural and tectonic controls of basin evolution in Southwestern Gondwana during the Phanerozoic. In: Tankard A.J. et al. (Eds.), Petroleum Basins of South America, Am. Assoc. Petroleum Geol., Memoir, 62:5–52, 1996.

[9] Milani E.J., Evolução tectono-estratigráfica da Bacia do Paraná e seu relacionamento com a geodinâmica fanerozóica do Gondwana Sul-Ocidental, Ph.D. Thesis, Federal University of Rio Grande do Sul, 1997, 255p.

[10] Johnston S.T., The Cape Fold Belt and Syntaxis, and the rotated Falkland Islands: dextral transpressional tectonics along the southwest margin of Gondwana, J. African Earth Sc., 31:51–63, 2000.

[11] Riccomini C., Velázquez V.F., Gomes C.B., Tectonic controls of the Mesozoic and Cenozoic alkaline magmatism in central-southeastern Brazilian platform. In: Comin-Chiaramonti P., Gomes C.B. (Eds.), Mesozoic to Cenozoic alkaline magmatism in the Brazilian Platform, Edusp/Fapesp, São Paulo, 2005, pp. 31–56.
[12] Fisseha S., Ussami N., Padilha A.L., Vitorello I., Crustal structures of Cenozoic Pantanal wetland (SW Brazil) from MT and gravity studies: geophysical evidence of a buried Neoproterozoic-Cambrian suture zone, Am. Geophys. Union, Fall Meeting, Abstract, GP11A-0254F.
[13] Kröner A., Cordani U.G., African, southern Indian and South AmericanCratons were not part of the Rodinia supercontinent: evidence from field relationships and geochronology, Tectonophysics, 375:325–352, 2003.
[14] Cordani U.G., Teixeira W., D'Agrella Filho M.S., Trindade R.I., The position of the Amazonian Craton in supercontinents, Gondwana Res., 15:396–407, 2009.
[15] Comin-Chiaramonti P., Marzoli, A., Gomes C.B., Milan A., Riccomini C., Velázquez V.F., Mantovani M.M.S., Renne P., Tassinari C.C.G., Vasconcelos P.M., The origin of post-Paleozoic magmatism in eastern Paraguay, Geol. Soc. Am., Sp. Paper, 430:603–633, 2007.
[16] Almeida F.F.M., Geologia do Sudoeste Matogrossense, Div. Geol. Min., DNPM, Bol. 116, 118 p., 1945.
[17] Ussami N., Shiraiwa S., Dominguez J.M.L., Basement reactivation in a sub-Andean foreland flexural bulge: the Pantanal wetland, SW Brazil. Tectonics, 18:25–39, 1999.
[18] Paranhos Filho A.C., Nummer A.R., Albrez E.A., Ribeiro A.A., Machado R., 1013, A study of structural lineaments in Pantanal (Brazil) using remote sensing data, An. Acad. Brasil. Cienc. 85: 913–922.
[19] Gomes C.B., Laurenzi M.A., Censi P., De Min A., Velázquez V.F., Comin-Chiaramonti P., Alkaline magmatism from northern Paraguay (Alto Paraguay): a Permo-Triassic province. In: Comin-Chiaramonti P., Gomes C.B. (Eds.), Alkaline magmatism in central-eastern Paraguay. Relationships with coeval magmatism in Brazil, Edusp/Fapesp, São Paulo, 1996, pp. 208–222.
[20] Comte D., Hasui Y., Geochronology of Eastern Paraguay by the potassium-argon method, Rev. Bras. Geoc., 1:33–43, 1971.
[21] Sonoki I.K., Garda G.M., Idades K/Ar de rochas alcalinas do Brasil Meridional e Paraguai Oriental: compilação e adaptação às novas constantes de decaimento, Bol. IG-USP, Sér. Cient., 19:63–87, 1988.
[22] Velázquez V.F., Gomes C.B., Teixeira W., Comin-Chiaramonti P., Contribution to the geochronology of the Permo-Triassic alkaline magmatism from the Alto Paraguay Province, Rev. Bras. Geoc., 26:103–108, 1996.
[23] Kirschvink J.L., The least-squares line and plane and the analysis of paleomagnetic data, Geophys. J. R. Astron. Soc., 62:699–718, 1980.
[24] Fisher R.A., Dispersion on a sphere, Proceendings of Royal Society of London, Ser. A 217, 295–305, 1953.
[25] Domeier D., Van der Voo R., Tohver E., Tomezzoli R.N., Vizan H., Torsvik T.H., New Late Permian paleomagnetic data from Argentina: refinement of the apparent polar wander path of Gondwana, G3 12, Q07002, 2011, doi:10.1029/2011GC003616.
[26] Yokoyama E., Brandt D., Tohver E., Trindade R., The Pangea conundrum: implications of a new paleomagnetic pole from the Permo-Triassic Araguainha impact structure (Central Brazil), Latinmag Lett., 3:PB16, 1–6, Proceedings, Montevideo, 2013, Uruguay.
[27] Cañon-Tapia E., Pinkerton H., The anisotropy of magnetic susceptibility of lava flows: an experimental approach, J. Volc. Geotherm. Res., 98:219–233, 2000.
[28] Bascou J., Camps P., Dautria J.M., Magnetic versus crystallographic fabrics in a basaltic lava flow, J. Volc. Geotherm. Res., 145:119–135, 2005.
[29] Tamrat E., Ernesto M., Paleomagnetic constraints on the age of the Botucatu Formation in Rio Grande do Sul, Southern Brazil, An. Acad. Bras. Ciênc., 78:1–15, 2006.
[30] Kent V.D., Olsen P., Astronomically tuned geomagnetic time scale for the Late Triassic, J. Geophys. Res., 104:12831–12841, 1999.
[31] Gomes C.B., Comin-Chiaramonti P., Velázquez V.F., A synthesis on the alkaline magmatism of Eastern Paraguay, Brazilian J. Geol., 43:745–761, 2013.
[32] Brandt D., Ernesto M., Rocha-Campos A.C., Santos P.R., Paleomagnetism of the Santa Fé Group, central Brazil: implications for the late Paleozoic apparent polar wander path for South America, J. Geophys. Res., 114, p. B02101, 2009.
[33] Domeier M., Van der Voo R., Torsvik T.H., Paleomagnetism and Pangea: the road to reconciliation, Tectonophysics, 514-517:14–43, 2012.